DETERMINATION OF THREE-DIMENSIONAL VELOCITY ANOMALIES UNDER A SEISMIC ARRAY USING FIRST P ARRIVAL TIMES FROM LOCAL EARTHQUAKES
1. A HOMOGENEOUS INITIAL MODEL

Keiiti Aki

Department of Earth and Planetary Sciences, Massachusetts Institute of Technology, Cambridge, Massachusetts 02139

W. H. K. Lee

National Center for Earthquake Research, U. S. Geological Survey
Menlo Park, California 94025

Abstract. Geiger's method of locating local earthquakes has been extended to include the effect of P velocity variation along the ray paths in three dimensions. The crustal structure was modeled by rectangular blocks, and a parameter was assigned to each block describing the perturbation of P wave slowness in the block. On the basis of an initial model, a set of linear equations for the observed first P arrival times was formulated in terms of the source and medium parameters. The source parameters for all the earthquakes in the data set and medium parameters for all the blocks penetrated by the seismic rays were then determined simultaneously by the damped least squares method. A computer program has been written for the case of a homogeneous initial medium model with constant P velocity. It has been tested with artificial data and applied to a set of local earthquakes recorded by a dense seismic array in Bear Valley, California. The resultant velocity distribution in the top 5 km shows a narrow low-velocity zone of about 5km/s in the San Andreas fault zone sandwiched between high-velocity regions of about 6 km/s.

Introduction

The principal data gathered in a microearthquake monitoring network of seismograph stations such as that operated by the U. S. Geological Survey in central California, are first P arrival times from local earthquakes. These data contain information on both tectonics and structure of the earth under the network. In addition to four source parameters (epicenter coordinates, focal depth, and origin time), each earthquake event contributes independent observations, as much as the number of observed stations in excess of 4, to the potential data set for determining the earth's structure. Recently, Crosson [1974] demonstrated the usefulness of local earthquake data in the study of crustal structure under western Washington. In the present paper we shall present a powerful method of extracting the crustal structure information from the first P arrival time data by incorporating a new earth modeling technique in the hypocenter location program of local earthquakes.

Copyright 1976 by the American Geophysical Union.

Following Aki et al., [1976] we shall divide the earth under a seismograph network into blocks and assign a parameter to each block describing the perturbation of seismic wave slowness in the block. In this paper we call it the slowness perturbation or medium parameter. Assuming an initial model, we formulate a set of linearized equations for the observed first P arrival times in terms of the source and medium parameters. The source parameters (for all the earthquakes in the data set) and medium parameters (for all the blocks penetrated by the seismic rays) are determined simultaneously by an appropriate inversion technique.

For simplicity, we assume a homogeneous initial model of constant P velocity. We start with a set of earthquakes with initial hypocenter locations and origin times and ask what changes have to be made to the initial source and medium parameters such that the observed P arrival times are best fitted in a least squares sense. In future papers we plan to remove the restriction of a homogeneous initial model by using ray-tracing techniques in a heterogeneous medium.

We shall first test our method by using artificial data generated for known source and medium and examine the effectiveness of our measures for resolution and error. We shall then apply our method to a set of earthquake data obtained by the U.S. Geological Survey's Bear Valley experiment [Fischer et al.,1975]. With a block size of 3 x 4 x 5 km the resultant velocity structure shows remarkable correlation with fault traces and surface geology.

The approach that we use in this paper is a first step toward a systematic analysis of

Table 1. Locations of Earthquakes for Artificial Data Set 3

Earthquake Number	X, km	Y, km	Z, km
1	12.0	7.0	6.0
2	12.0	12.0	6.0
3	12.0	17.0	6.0
4	12.0	22.0	6.0
5	12.0	27.0	6.0
6	12.0	32.0	6.0

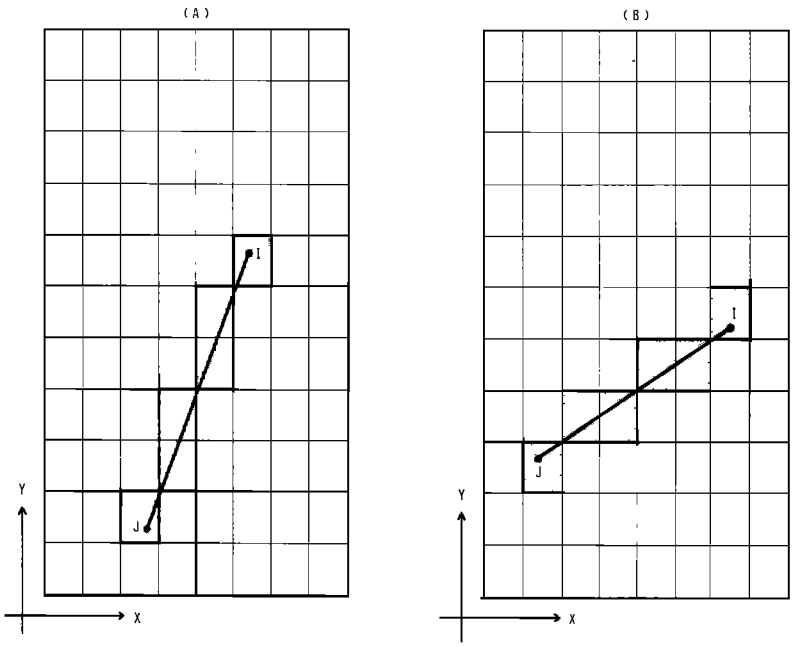

Fig. 1. Sampling of blocks along a ray path for the cases in which the horizontal distance exceeds the vertical distance.

local earthquake data. The method can be extended in two directions by (1) increasingly more realistic modeling of seismic rays between source and station and (2) incorporating later P arrival and S arrival times as well as amplitude data in the inversion. Our goal is to deduce parameters that characterize the medium along ray paths with greater spatial resolution and accuracy from the observations. With improved resolution and accuracy our method will enable the detection of precursory velocity change, if any, for smaller earthquakes. Since smaller earthquakes are more frequent, we shall be able to test methods for earthquake prediction in a shorter time.

Formulation of the Problem

Since the area of study is small in comparison with the earth's surface area, we shall use a Cartesian coordinate system with the Z axis vertically downward and we shall write the station coordinates as X_i, Y_i, and Z_i ($i = 1, 2, \ldots, N$). Consider a volume of the earth under the station network and divide it into equal rectangular blocks with sides parallel to the X, Y, and Z axes. The side lengths in the X, Y, and Z directions are S_x, S_y, and S_z, respectively.

Our data consist of first P arrival times observed at N stations from a set of M earthquakes. We denote the first P arrival time from the jth earthquake observed at the ith station as T_{ij}^{obs}. In order to formulate a set of linear equations for the observed data in terms of source and medium parameters we shall make the following assumptions:

1. Initial guesses of the epicenter, focal depth, and origin times are known as X_j^o, Y_j^o, Z_j^o, and T_j^o, respectively, for $j = 1, 2, \ldots, M$. The initial locations are all inside the volume of our block model.
2. For simplicity, we shall assume a homogeneous half space with a constant P velocity V_o as the initial earth model.

We can then write the equation for an observed

Table 2. Locations of Earthquakes Determined by HYPO71 and Our Program From Data Set 3 Without Random Errors

Earthquake Number	HYPO71			Our Method		
	X	Y	Z	X	Y	Z
1	9.42	7.25	5.00	12.01	7.02	5.96
2	9.57	12.00	5.00	11.99	12.00	5.96
3	9.49	16.88	6.17	11.99	16.98	6.02
4	9.71	22.08	5.56	11.99	22.00	6.01
5	9.77	26.92	5.61	12.00	27.00	6.00
6	9.52	31.85	5.56	12.00	32.01	5.99

X, Y, and Z are in kilometers.

Table 3. Locations of Earthquakes With Standard Errors Determined by the Undamped Least Squares Method Using Data Set 3 With Random Errors

Earthquake Number	X, km	Y, km	Z, km
1	11.95 ± 0.17	7.05 ± 0.20	5.80 ± 0.42
2	11.92 ± 0.10	11.84 ± 0.14	5.73 ± 0.32
3	11.74 ± 0.11	16.76 ± 0.10	6.16 ± 0.30
4	11.98 ± 0.15	22.10 ± 0.08	6.03 ± 0.29
5	12.11 ± 0.12	26.94 ± 0.11	5.66 ± 0.31
6	11.82 ± 0.14	31.83 ± 0.17	5.77 ± 0.37

Table 4. Slowness Perturbation in Percent With the Standard Error for Layer 1 Obtained by the Undamped Least Squares Method Using Data Set 3 With Random Errors

Block Number in Y Direction	Block Number in X Direction							
	1	2	3	4	5	6	7	8
1	2 ± 10	-14 ± 9	-14 ± 9	-21 ± 12	12 ± 12	4 ± 9	14 ± 9	2 ± 10
2	-16 ± 6	-11 ± 5	-8 ± 5	-6 ± 7	8 ± 7	11 ± 5	6 ± 5	4 ± 6
3	-9 ± 7	-9 ± 3	-8 ± 3	-9 ± 3	8 ± 3	10 ± 3	13 ± 3	12 ± 7
4	-19 ± 9	-11 ± 3	-6 ± 2	-7 ± 2	10 ± 2	10 ± 2	8 ± 3	6 ± 9
5	-17 ± 9	-8 ± 3	-7 ± 2	-7 ± 2	10 ± 2	10 ± 2	8 ± 3	12 ± 9
6	-21 ± 9	-7 ± 4	-7 ± 2	-12 ± 2	9 ± 2	11 ± 2	9 ± 4	20 ± 9
7	-10 ± 9	-8 ± 3	-9 ± 2	-10 ± 2	7 ± 2	10 ± 2	9 ± 3	2 ± 9
8	-11 ± 9	-15 ± 3	-6 ± 2	-9 ± 2	9 ± 2	11 ± 2	7 ± 3	16 ± 9
9	3 ± 9	-7 ± 3	-9 ± 2	-6 ± 2	13 ± 2	12 ± 2	5 ± 3	13 ± 9
10	0 ± 7	-15 ± 4	-8 ± 3	-6 ± 3	9 ± 4	8 ± 3	6 ± 3	8 ± 7
11	5 ± 8	-3 ± 6	-6 ± 6	-14 ± 8	18 ± 8	18 ± 6	11 ± 6	14 ± 8

first P arrival time as

$$T_{ij}^{obs} = T_{ij}^{cal} + \left(\frac{\partial T}{\partial X}\right)_{ij} \Delta X_j + \left(\frac{\partial T}{\partial Y}\right)_{ij} \Delta Y_j + \left(\frac{\partial T}{\partial Z}\right)_{ij} \Delta Z_j + \Delta T_j + \sum_k T_{ij}^{(k)} F_k + E_{ij} \quad (1)$$

where T_{ij}^{cal} is the calculated first P arrival time based on the homogeneous initial model:

$$T_{ij}^{cal} = T_j^o + \left[(X_i - X_j^o)^2 + (Y_i - Y_j^o)^2 + (Z_i - Z_j^o)^2\right]^{1/2}/V_o \quad (2)$$

Table 5. Slowness Perturbation in Percent With the Standard Error for Layer 2 Obtained by the Undamped Least Squares Method Using Data Set 3 With Random Errors

Block Number in Y Direction	Block Number in X Direction	
	4	5
3	-8 ± 7	9 ± 7
4	-7 ± 4	12 ± 4
5	-4 ± 5	16 ± 4
6	-10 ± 5	12 ± 5
7	-7 ± 4	0 ± 4
8	-7 ± 4	13 ± 4
9	-3 ± 4	13 ± 4
10	-14 ± 8	10 ± 7

The derivatives of travel time with respect to the X, Y, and Z coordinates are also calculated for the homogeneous initial model as

$$\left(\frac{\partial T}{\partial X}\right)_{ij} = -(X_i - X_j^o)/V_o^2 (T_{ij}^{cal} - T_j^o)$$
$$\left(\frac{\partial T}{\partial Y}\right)_{ij} = -(Y_i - Y_j^o)/V_o^2 (T_{ij}^{cal} - T_j^o) \quad (3)$$
$$\left(\frac{\partial T}{\partial Z}\right)_{ij} = -(Z_i - Z_j^o)/V_o^2 (T_{ij}^{cal} - T_j^o)$$

The terms ΔX_j, ΔY_j, ΔZ_j, and ΔT_j are corrections to the source parameters of the jth earthquake.

The sixth term on the right-hand side of (1) expresses the travel time variation due to the perturbation of wave slowness. F_k represents the fractional perturbation of slowness in block k from the initial value V_o^{-1}, i.e., $F_k = (V^{-1} - V_o^{-1}) / V_o^{-1} \doteq -(V - V_o)/V_o$. Along a given ray path (i, j) connecting the ith station with the initial location of the jth earthquake we find which blocks are penetrated by the ray path and also calculate the travel time spent by the ray in each of the blocks. Thus $T_{ij}^{(k)}$ is the time spent in block k by the ray (i, j), and the summation is made over all blocks penetrated by the ray (i, j). Some simplification is made on the actual block sampling as described later. Finally, E_{ij} in (1) represents the higher-order terms and errors in observation.

To make (1) compact, we shall write the whole set of observed minus calculated P arrival times

Table 6. Locations of Earthquakes With Standard Errors by the Damped Least Squares Method Using Data Set 3 With Random Errors

Earthquake Number	X, km	Y, km	Z, km
1	11.77 ± 0.07	7.02 ± 0.07	5.91 ± 0.13
2	11.86 ± 0.07	11.94 ± 0.07	5.85 ± 0.14
3	11.76 ± 0.07	16.86 ± 0.06	6.03 ± 0.14
4	11.86 ± 0.07	22.07 ± 0.06	5.98 ± 0.14
5	11.98 ± 0.08	26.96 ± 0.06	5.81 ± 0.14
6	11.72 ± 0.07	31.93 ± 0.07	5.89 ± 0.13

as a column vector τ, with components arranged as follows:

$$\tilde{\tau} = (\tau_{11}, \tau_{21}, \ldots, \tau_{N1}, \tau_{12}, \tau_{22}, \ldots, \tau_{N2}, \ldots \tau_{NM})$$

where $\tau_{ij} = T_{ij}^{obs} - T_{ij}^{cal}$, and $\tilde{\tau}$ denotes the transpose of τ. We also write the entire source and medium parameters as a column vector χ, with components arranged as follows:

$$\tilde{\chi} = (\Delta X_1, \Delta Y_1, \Delta Z_1, \Delta T_1, \ldots, \Delta X_M, \Delta Y_M, \Delta Z_M, \Delta T_M, F_1, F_2, \ldots F_K)$$

Then (1) can be rewritten as

$$\tau = G\chi + \varepsilon \qquad (4)$$

where ε is an error vector with components E_{ij} and G is a NM x (4M + K) matrix with the components given in (1). Since only four source parameters and a small number of medium parameters for blocks lying along a particular ray path contribute to each of the observed first P arrival times, most of the elements of matrix G are zero.

Damped Least Squares Solution

The least squares solution of (4) satisfies the normal equation

$$\tilde{G}G\chi = G\tau \qquad (5)$$

where $\tilde{G}$ is the transpose of G. In the case of the teleseismic data to which the block model was first applied by Aki et al., [1976], the matrix $\tilde{G}G$ was always singular, and the solution of (5) was nonunique. This was due to the particular initial model used by them, which consisted of flat layers and the assumption of a plane wave source. The observation made on the horizontal surface could not distinguish the effect of a slowness perturbation uniform in a layer from the effect of, say, a change in origin time of the plane wave source. Additional sources of nonuniqueness occurred when data were insufficient and any pair of blocks always shared common ray paths. In this case, the observation could not distinguish the effect of perturbation in one block of the pair from the other, and the solution became nonunique.

At first glance, the nonuniqueness problem may seem even worse in our case of local earthquake data because of the additional unknown source parameters. For example, if a block containing a hypocenter is never penetrated by rays from other earthquakes, we anticipate the difficulty of distinguishing the effect of slowness perturbation for the block from that of change in origin time of the earthquake in the block. However, this nonuniqueness can be removed by the use of a large amount of data because unlike the case of teleseismic data, strictly speaking, there is a slight difference between the effects of the above two

Table 7. Slowness Perturbation in Percent With the Standard Error for Layer 1 Obtained by the Damped Least Squares Method Using Data Set 3 With Random Errors

Block Number in Y Direction	Block Number in X Direction							
	1	2	3	4	5	6	7	8
1	-1 ± 3	-6 ± 3	-4 ± 3	-6 ± 2	5 ± 2	2 ± 3	6 ± 3	2 ± 3
2	-10 ± 3	-9 ± 2	-9 ± 2	-9 ± 2	9 ± 2	11 ± 2	7 ± 2	5 ± 3
3	-4 ± 3	-8 ± 2	-8 ± 2	-8 ± 2	9 ± 2	10 ± 2	11 ± 2	6 ± 3
4	-5 ± 3	-10 ± 2	-6 ± 2	-7 ± 1	9 ± 1	10 ± 2	8 ± 2	1 ± 3
5	-4 ± 3	-9 ± 2	-7 ± 2	-7 ± 1	9 ± 1	9 ± 2	9 ± 2	4 ± 3
6	-6 ± 3	-8 ± 2	-7 ± 2	-11 ± 1	9 ± 1	11 ± 2	9 ± 2	7 ± 3
7	-2 ± 3	-8 ± 2	-9 ± 2	-9 ± 1	9 ± 1	10 ± 2	10 ± 2	-1 ± 3
8	-3 ± 3	-11 ± 2	-7 ± 2	-9 ± 1	9 ± 1	10 ± 2	7 ± 2	6 ± 3
9	0 ± 3	-5 ± 2	-9 ± 2	-8 ± 2	12 ± 1	11 ± 2	7 ± 2	4 ± 3
10	-3 ± 3	-11 ± 2	-7 ± 2	-6 ± 2	10 ± 2	8 ± 2	7 ± 2	4 ± 3
11	-1 ± 3	-3 ± 3	-3 ± 3	-6 ± 3	8 ± 3	10 ± 3	7 ± 3	6 ± 3

Table 8. Slowness Perturbation in Percent With the Standard Error for Layer 2 Obtained by the Damped Least Squares Method Using Data Set 3 With Random Errors

Block Number in Y Direction	Block Number in X Direction	
	4	5
3	-4 ± 3	5 ± 3
4	-9 ± 2	11 ± 2
5	-7 ± 2	13 ± 2
6	-10 ± 3	11 ± 3
7	-8 ± 2	4 ± 2
8	-8 ± 2	14 ± 2
9	-7 ± 2	12 ± 2
10	-7 ± 3	8 ± 3

factors on the observations. If we have sufficient data therefore, we have no reason to expect the matrix $\tilde{G}G$ to be singular. The examples given later in this paper show that $\tilde{G}G$ is in fact nonsingular and a unique solution of (5) can be obtained. In practice, however, some of the eigenvalues of $\tilde{G}G$ can be very small if the effects of any two different parameters are practically indistinguishable from the observations. In such a case, small random errors in data can cause strong fluctuation in the solution. One way of suppressing the undesirable effect of small eigenvalues is to modify the normal equation (5) to the following form

$$(\tilde{G}G + \Theta)\,\hat{\chi} = \tilde{G}\tau \qquad (6)$$

where Θ is a diagonal matrix with positive elements θ_i. The solution of (6) was called 'damped least squares' by Levenberg [1944] and can be obtained by minimizing $|\tau - G\chi|^2 + \tilde{\chi}\Theta\chi$ instead of $|\tau - G\chi|^2$. In other words, the sum of the squares of the data residual and the weighted sum of the squares of solution components are minimized to obtain the estimate $\hat{\chi}$. If we consider both data τ and solution χ as independent Gaussian variables, the maximum likelihood estimate of the solution would be the weighted least squares estimate, with the weight inversely proportional to the variance. When the variance of τ is σ^2 and the variance of the ith component of χ is σ_i^2, the appropriate choice of the weight matrix is then,

$$\Theta = \begin{pmatrix} \sigma^2/\sigma_1^2 & 0 & 0 & \cdots \\ 0 & \sigma^2/\sigma_2^2 & 0 & \cdots \\ 0 & 0 & \sigma^2/\sigma_3^2 & \cdots \\ \cdots & \cdots & \cdots & \cdots \end{pmatrix} \qquad (7)$$

The same choice of Θ is obtained by the method of 'stochastic inverse' [Franklin, 1970] in which the inverse operator is determined to minimize the residual in the solution space instead of the usual data space.

Our estimate $\hat{\chi}$ can be written in terms of the least squares solution χ, using (5) and (6), as

$$\begin{aligned} \hat{\chi} &= (\tilde{G}G + \Theta)^{-1}\,\tilde{G}\tau \\ &= (\tilde{G}G + \Theta)^{-1}\,\tilde{G}G\chi \end{aligned} \qquad (8)$$

The resolving kernel or resolution matrix discussed by Backus and Gilbert [1968] and Wiggins [1972] is therefore in this case

$$R = (\tilde{G}G + \Theta)^{-1}\,\tilde{G}G \qquad (9)$$

If R is the identity matrix I, the solution is unique. The resolution gets poorer as R deviates from I. The magnitude of the diagonal element is a good measure of the resolution as shown by Wiggins [1972].

The random error in data τ will produce errors in our solution. Since the error $\Delta\hat{\chi}$ in the solution is related to error $\Delta\tau$ in data by (6), we can write the covariance matrix of $\Delta\hat{\chi}$ as

$$\begin{aligned} D = \langle\Delta\hat{\chi}\cdot\Delta\tilde{\hat{\chi}}\rangle &= (\tilde{G}G + \Theta)^{-1}\,\tilde{G}\langle\Delta\tau\Delta\tilde{\tau}\rangle \\ &\quad G(\tilde{G}G + \Theta)^{-1} \end{aligned} \qquad (10)$$

For $\langle\Delta\tau\Delta\tilde{\tau}\rangle = \sigma^2 I$, the above equation is simplified to

$$D = \sigma^2(\tilde{G}G + \Theta)^{-1}\,\tilde{R} \qquad (11)$$

The solution $\hat{\chi}$, the resolution matrix R, and the covariance matrix D can be obtained by operating the same matrix $(\tilde{G}G + \Theta)^{-1}$ as shown in (6), (9), and (11).

The variance σ^2 of errors in the data is estimated by the sum of the squared residuals $|\tau - G\hat{\chi}|^2$ divided by the number of degrees of freedom (NM - 4M - K). Since in the damped least squares we minimize $|\tau - G\chi|^2 + \tilde{\chi}\Theta\chi$ instead of $|\tau - G\chi|^2$, our estimate is a conservative overestimate of the true variance of errors in the data [Zandt 1975].

The choice of weight matrix Θ is determined by (7) by using an a priori guess on the root mean square (rms) level of the solution. For example, if the standard error of the time measurement is 0.1 s and the standard level of the fractional slowness fluctuation is 0.05, then the corresponding diagonal element of Θ is $0.01/0.0025 = 4\ s^2$. If the expected mean square levels of ΔX_j, ΔY_j, ΔZ_j, and ΔT_j are σ_x^2, and σ_y^2, σ_z^2, and σ_T^2, respectively, the corresponding diagonal elements of θ are chosen as $\theta_x = \sigma^2/\sigma_x^2$, $\theta_y = \sigma^2/\sigma_y^2$, $\theta_z = \sigma^2/\sigma_z^2$, and $\theta_T = \sigma^2/\sigma_T^2$.

Table 9. Diagonal Elements of the Resolution Matrix for the Source Parameters Determined by the Damped Least Squares Method Using Data Set 3

Earthquake Number	X	Y	Z	T
1	0.64	0.56	0.46	0.94
2	0.76	0.69	0.52	0.95
3	0.74	0.81	0.55	0.96
4	0.65	0.85	0.58	0.96
5	0.71	0.80	0.55	0.96
6	0.71	0.64	0.49	0.95

Table 10. Diagonal Elements of the Resolution Matrix for the Slowness Perturbation in Layer 1 Determined by the Damped Least Squares Method Using Data Set 3

Block Number In Y Direction	Block Number in X Direction							
	1	2	3	4	5	6	7	8
1	0.35	0.39	0.37	0.28	0.27	0.37	0.39	0.35
2	0.53	0.74	0.78	0.66	0.66	0.77	0.75	0.53
3	0.47	0.80	0.87	0.86	0.85	0.87	0.80	0.47
4	0.38	0.81	0.89	0.92	0.92	0.90	0.81	0.38
5	0.38	0.82	0.91	0.92	0.92	0.91	0.82	0.38
6	0.40	0.81	0.91	0.92	0.92	0.91	0.81	0.40
7	0.40	0.82	0.92	0.93	0.93	0.92	0.82	0.40
8	0.38	0.82	0.91	0.93	0.93	0.91	0.81	0.39
9	0.39	0.81	0.90	0.92	0.92	0.90	0.82	0.39
10	0.48	0.77	0.83	0.83	0.82	0.83	0.78	0.49
11	0.38	0.51	0.56	0.39	0.39	0.55	0.52	0.38

Table 11. Diagonal Elements of the Resolution Matrix for the Slowness Perturbation in Layer 2 Determined by the Damped Least Squares Method Using Data Set 3

Block Number In Y Direction	Block Number in X Direction	
	4	5
3	0.48	0.48
4	0.78	0.78
5	0.70	0.70
6	0.67	0.67
7	0.70	0.70
8	0.80	0.80
9	0.80	0.79
10	0.45	0.51

We shall describe later the effects of Θ on the solution, resolution, and error by using some artificial data as examples.

Computer Program

A computer program was written in Fortran to find the damped least squares solution together with the resolution and covariance matrix given by (6), (9), and (11). The input data to the program are the station coordinates, the initial source parameters, the observed first P arrival times for a set of local earthquakes, and specifications for the initial crustal structure model. The crustal model is specified by the block size and number of blocks in X, Y, and Z directions and assumes a constant P velocity, V_o, for all blocks initially.

The sampling of blocks along a given ray path was made as follows. First, the horizontal and vertical distances between the ith station and the jth earthquake hypocenter are compared. If the vertical distance is greater than the horizontal distance, we follow the method used by Aki et al., [1976] and sample one block from each layer. The block which contains most of the ray path within each layer is selected, and the travel time within the layer is calculated to be used as $T_{ij}^{(k)}$ in (1). For blocks at both ends of a ray path, $T_{ij}^{(k)}$ is the travel time over the length of ray segment terminated at each end.

When the vertical distance is less than the horizontal distance, we consider the following two cases separately. If the Y component of the horizontal distance is greater than the X component, we select one block from each layer with constant Y, as shown in Figure 1a. The procedure is identical to the method used by Aki et al., [1976] except that the Y axis plays the role of Z axis. Similarly, if the X component of the horizontal distance is greater than the Y component, we sample one block from each layer of constant X, as shown in Figure 1b.

We could have sampled all the blocks penetrated by a given ray and calculated exactly the travel time within each block. We have chosen this simplified method instead primar-

Table 12. Locations of Earthquakes Determined by the Damped Least Squares Method Using the Wrong Initial Earthquake Locations Given by HYPO71 (Table 2)

Earthquake Number	X, km	Y, km	Z, km
1	10.49 ± 0.12	7.19 ± 0.12	5.17 ± 0.21
2	10.85 ± 0.11	12.06 ± 0.12	5.46 ± 0.22
3	10.95 ± 0.12	16.92 ± 0.11	6.21 ± 0.22
4	11.08 ± 0.11	22.09 ± 0.10	5.81 ± 0.22
5	11.20 ± 0.11	26.87 ± 0.10	5.97 ± 0.23
6	10.74 ± 0.12	31.75 ± 0.12	6.11 ± 0.22

Table 13. Slowness Perturbation in Percent for Layer 1 Determined by the Damped Least Squares Method Using the Wrong Initial Earthquake Location Given by HYPO71 (Table 2)

Block Number in Y Direction	Block Number in X Direction							
	1	2	3	4	5	6	7	8
1	-1 ± 4	-5 ± 4	-6 ± 4	-12 ± 4	27 ± 4	-7 ± 5	11 ± 4	-2 ± 4
2	-11 ± 4	-8 ± 4	-10 ± 4	-6 ± 4	35 ± 4	2 ± 4	2 ± 4	6 ± 5
3	-5 ± 5	-6 ± 3	-7 ± 3	-17 ± 3	25 ± 3	4 ± 3	4 ± 4	9 ± 4
4	-6 ± 5	-4 ± 3	-6 ± 2	-8 ± 2	18 ± 3	3 ± 3	-4 ± 4	-1 ± 4
5	0 ± 5	-6 ± 3	-8 ± 2	-3 ± 2	22 ± 2	4 ± 3	2 ± 4	0 ± 4
6	-1 ± 5	-4 ± 3	-8 ± 2	-4 ± 2	24 ± 2	6 ± 3	-3 ± 4	2 ± 4
7	4 ± 5	-5 ± 3	-12 ± 2	-3 ± 2	22 ± 2	5 ± 3	-1 ± 4	-6 ± 4
8	2 ± 5	-7 ± 3	-8 ± 2	-6 ± 2	23 ± 2	-1 ± 3	-2 ± 4	4 ± 4
9	-2 ± 5	-3 ± 3	-7 ± 2	-5 ± 2	21 ± 3	-3 ± 3	0 ± 4	4 ± 5
10	-4 ± 5	-9 ± 4	-6 ± 3	-24 ± 3	21 ± 3	-1 ± 4	1 ± 4	0 ± 4
11	-1 ± 5	-0 ± 5	-10 ± 4	-3 ± 4	38 ± 5	-1 ± 5	9 ± 5	-1 ± 4

ily because of the saving in computer time. This simplification may have some smoothing effect on the resultant medium parameters. The smoothing may blur the picture of the seismic anomaly pattern but will not distort it as long as a block is sampled by many rays with good azimuthal coverage.

Testing with Artificial Data

An obvious way of testing our computer program is to apply it to an artificial data set generated for a specified model of the source and medium. Actually, our computer program provides us with such a test internally in the form of the resolution matrix given in (9). The ith column vector of the resolution matrix is the solution $\tilde{\chi}$ of (6) corresponding to the data vector τ, which is generated for a model vector χ_i having only one nonvanishing element, i.e., the ith element.

Data set 1. To provide an external check, we generated several sets of artificial data of first P arrival times by using the HYPO71 computer program [Lee and Lahr, 1975]. In one case, we computed the travel times from hypocenters of eight sample earthquakes to 60 stations in the Bear Valley area in central California by assuming a homogeneous half space with a constant P velocity of 5.67 km/s. To approximate real data with observational errors, we added a random number of a boxcar distributions from -0.1 to +0.1 s (standard error of about 0.06 s) to each of the artificial first P arrival times.

We then inverted these artificial data with our program by dividing the earth under the Bear Valley station network into 264 cubic blocks 3 km on a side with the number of blocks 11 parallel to the San Andreas fault, 8 perpendicular to the San Andreas fault, and 3 deep having a homogeneous initial P velocity of 5.67 km/s. For our artificial data, 102 blocks out of a total of 264 blocks are penetrated by at least one seismic ray. The inversion was made by the damped least squares method with the same weight matrix Θ as used for inverting the actual data from Bear Valley.

Initially, the rms time residual was 0.069 s and it was slightly reduced to 0.062 s after the inversion. Representative corrections to the X, Y, and Z coordinates of hypocenter are 80, -10, and 420 m with the corresponding estimated standard errors of 150, 140, and 340. A typical correction to the origin time is 0.011 s with a standard error of 0.038 s. For six randomly selected blocks the slowness perturbations are -1.4, -2.5, -0.9, -3.2, -2.1, and 1.5% with corresponding standard errors of 1.1, 2.6, 2.5, 2.8, 2.6, and 2.5%. These results show that revisions of the initially assumed source and medium parameters are not required by this set of artificial data, as expected.

Data set 2. The HYPO71 program can also compute travel times in a horizontally flat layered medium. We generated a second set of artificial data exactly as the first data set, except for a medium consisting of three layers over a half space. Each layer is 3 km thick, and the P velocities for the first, second, and third layer are 4, 5, and 6 km/s, respectively. The underlying half space has a P velocity of 8 km/s. Since three events are located in the first layer, two in the second, and three in the third, most ray paths lie in the first and second layers. We therefore assumed the initial P velocity for all blocks to be the average of the first two layers, i.e., 4.5 km/s, in our inversion program. Again, the inversion was made by the damped

Table 14. Slowness Perturbation in Percent for Layer 2 Determined by the Damped Least Squares Method Using the Wrong Initial Earthquake Location Given by HYPO71 (Table 2)

Block Number In Y Direction	Block Number in X Direction	
	3	4
3		-13 ± 4
4	-6 ± 4	2 ± 4
5		4 ± 4
6		- 1 ± 4
7	-4 ± 4	-10 ± 4
8		- 6 ± 5

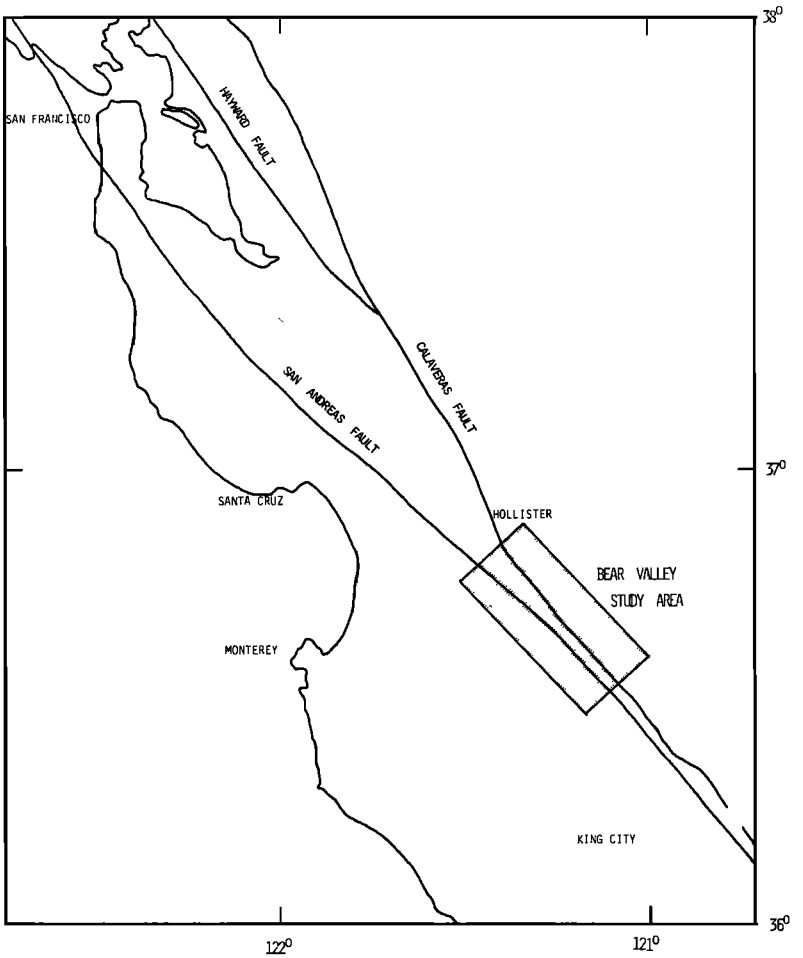

Fig. 2. Index map of central California showing the Bear Valley study area.

least squares method with the same weight matrix Θ as used for inverting the actual data from the Bear Valley.

The initial rms time residual was 0.26 s, and it was reduced to 0.08 after the inversion. The inversion result reveals a significant bias in the solution of both source and medium parameters. The medium parameters are determined with standard errors of 2 to 4% and show that the velocity in the first layer is significantly higher by about 10% than the average velocity of 4.5 km/s, whereas the true velocity for the first layer is 4 km/s. This bias is due to the fact that the artificial data generated from a layered medium contain refracted waves which are neglected in our simplified initial model of a homogeneous half space. Since source and medium parameters are coupled in (1), significant biases in source parameters are also introduced.

A similar bias is expected for a laterally inhomogeneous medium such as expected near the fault zones. It is therefore important to include the ray tracing in a three-dimensional heterogeneous medium in our computer program so that we can set up our basic linearized equation (1) for an inhomogeneous initial model.

Data set 3. Here, we shall consider only the simplest case of hypothetical lateral inhomogeneity in which the ray path is exactly a straight line. The medium is assumed to have a uniform velocity of 6.0 km/s to the west of the San Andreas fault and 5.0 km/s to the east and earthquakes are located on the fault. In this case we used the same block configuration as used for analyzing the actual data from the Bear Valley; the side lengths of blocks in the directions parallel (Y axis) and perpendicular (X axis) to the San Andreas fault are 4 and 3 km, respectively, and each layer with thickness 5 km is divided into 8 x 11 blocks (Figure 1). We shall set up an idealized seismic network with one station in each of the blocks, altogether 88 stations uniformly distributed over the area. Then, we generate artificial data for travel times at these stations for six earthquakes located on the San Andreas fault. Their locations are listed in Table 1.

At first, the above data set without random error was used to compare our inversion program with the conventional location program HYPO71. Our initial model is the homogeneous half space with a constant velocity 5.5 km/s. The same model was assumed for the HYPO71. The true location listed in Table 1 is used as the initial location by both programs. Since random errors are not included, we first tried the undamped least squares method in which the ele-

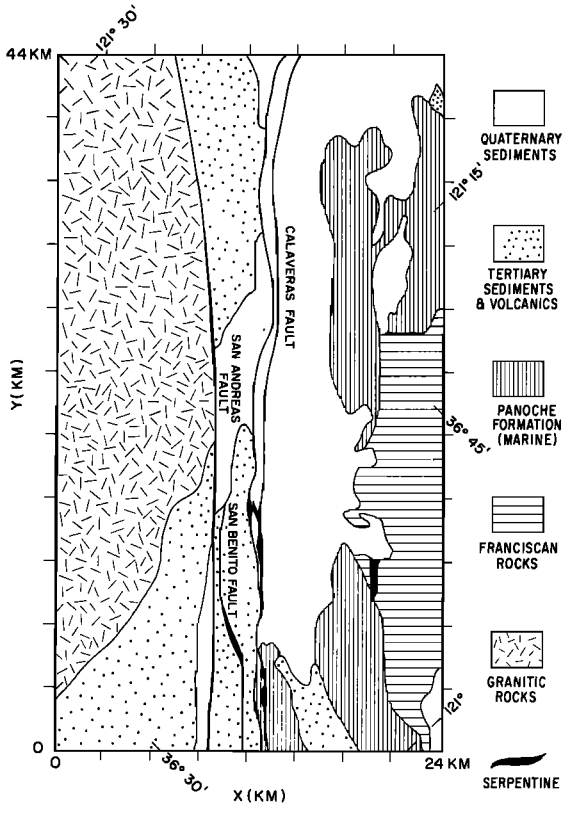

Fig. 3. Generalized geologic map of the Bear Valley study area.

ments of Θ are all zero. The results of inversion for source parameters are shown in Table 2. As expected, the epicenters obtained by HYPO71 are shifted to the west by about 2.5 km. On the other hand, our program gives an excellent result. The true locations are recovered with an error of less than 20 m for epicenter and less than 40 m for focal depth, which are probably due to the round off errors. The solutions for slowness perturbation lie in the range -0.080 to -0.090 on the west side and +0.095 to +0.105 on the east side. This is again a satisfactory result because the true slowness perturbation is -0.0833 on the west and +0.10 on the east. The diagonal elements of the resolution matrix are unity for all the blocks including those containing the hypocenter. Thus we confirm our earlier contention that we can obtain a unique solution of our problem when sufficient data are available.

Now, we add measurement errors simulated by the random number of a boxcar distribution from -0.1 to +0.1 s (standard error of about 0.06 s) to the above artificial data set. First, we shall show the solution for the case of undamped least squares ($\theta_i = 0$). The initial locations are again the ones given in Table 1, and the initial medium is a homogeneous body with velocity 5.5 km/s. The result of inversion for source parameters is quite satisfactory as given in Table 3. The standard errors are reasonably small, and we find no systematic shift of locations from the true ones. However, the solutions for the slowness

Table 15. Coordinates of Seismic Stations in the Bear Valley Study Area

Station Code	X, km	Y, km	Z, km
AB1	9.72	28.51	-0.24
AB2	9.62	27.72	-0.23
AB3	9.74	26.95	-0.22
AB4	9.89	26.18	-0.22
AB5	9.90	25.37	-0.26
AB6	9.87	24.58	-0.24
AB7	8.90	20.71	-0.58
BB1	7.56	21.63	-0.36
BB2	8.02	21.00	-0.34
BB3	8.03	20.30	-0.33
BB4	8.26	19.62	-0.31
BB5	8.94	19.26	-0.30
BB6	9.72	18.26	-0.28
BB7	10.22	17.64	-0.25
CB1	10.15	14.93	-0.28
CB2	10.33	13.75	-0.29
CB3	10.42	12.43	-0.30
CB4	10.02	11.82	-0.30
CB5	9.55	11.07	-0.39
CB6	9.16	10.32	-0.41
CB7	8.92	9.58	-0.45
DB1	8.42	8.10	-0.44
DB2	8.62	7.31	-0.43
DB3	8.74	6.09	-0.44
DB4	8.58	5.38	-0.41
DB5	8.36	4.22	-0.41
DB6	8.02	3.02	-0.38
DB7	7.66	1.87	-0.39
EB1	2.68	11.59	-0.64
EB2	3.92	11.28	-0.60
EB3	5.38	11.01	-0.57
EB4	6.37	10.41	-0.55
EB5	6.97	9.61	-0.53
EB6	7.43	8.85	-0.52
EB7	8.44	8.61	-0.44
LB1	2.52	14.45	-0.74
LB2	6.48	25.20	-0.76
LB5	5.36	12.24	-0.69
LB6	8.28	17.40	-0.73
MB1	5.75	30.58	-0.67
MB2	2.96	23.10	-0.83
MB5	3.25	27.09	-1.02
MB6	5.95	22.24	-0.90
TPBV	19.67	23.23	-0.49
TPCM	19.69	5.48	-1.18
TPCS	13.48	12.12	-0.77
TPER	15.70	16.48	-0.37
TPMC	17.43	19.85	-0.28
TPPC	22.13	4.18	-0.86
TPPP	12.72	8.50	-0.72
TPSA	20.58	26.54	-0.44
TPSC	16.53	6.60	-0.63
BGM	20.60	1.08	-1.22
BVL	8.65	9.73	-0.51
CNR	8.67	30.02	-0.30
EKH	16.39	16.10	-0.34
EMM	21.26	11.07	-0.49
JON	3.19	20.21	-1.05
LWR	10.03	22.21	-0.23
STC	10.27	17.30	-0.26

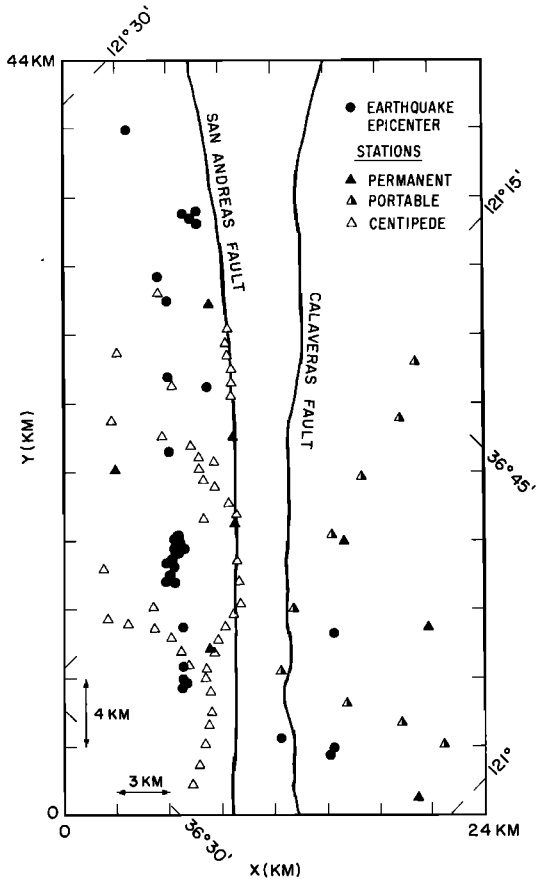

Fig. 4. Map showing seismic stations and earthquake epicenters determined from a regional crustal model (case 1).

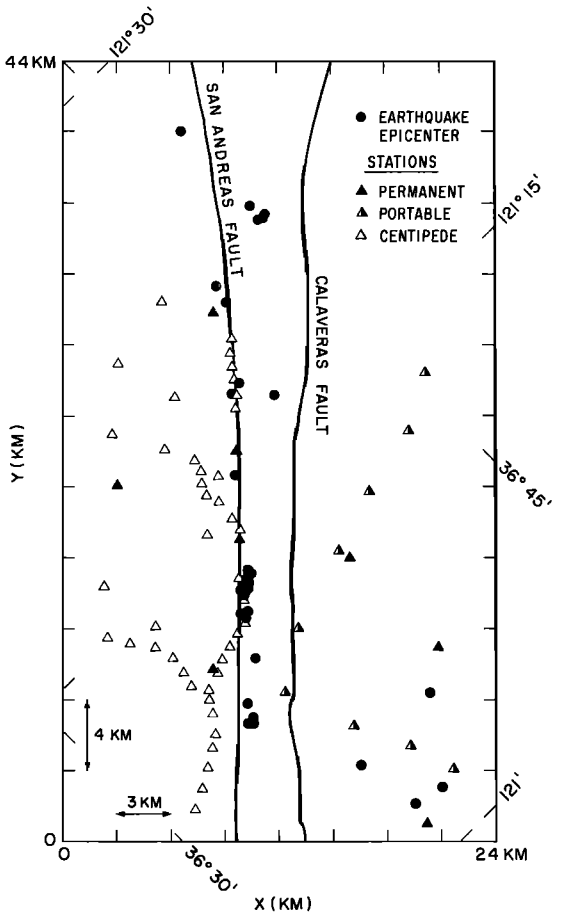

Fig. 5. Map showing seismic stations and earthquake epicenters determined from a local crustal model (case 2).

perturbation have too large standard errors as shown in Table 4 for layer 1 (0 to 5 km depth) and in Table 5 for layer 2 (5 to 10 km depth). The standard errors for blocks in the peripheral area amount to 10%, although they are small (≈2%) for interior blocks.

Now, we use the damped least squares method to suppress the effect of random error. Choosing the rms levels of slowness fluctuation, epicenter coordinates, focal depth, and origin time as 0.06, 0.2 km, 0.3 km, and 0.12 s, respectively, and since $\sigma = 0.06$ s, the diagonal elements of the weight matrix Θ are set as: slowness perturbation

$$\Theta_i = 1 \text{ s}^2 \tag{12a}$$

epicenter coordinates

$$\Theta_x = \Theta_y = 0.11 \text{ s}^2/\text{km}^2 \tag{12b}$$

focal depth

$$\Theta_2 = 0.04 \text{ s}^2/\text{km}^2 \tag{12c}$$

origin time

$$\Theta_T = 0.25 \tag{12d}$$

We assume again the true hypocenter to be the initial location and the homogeneous body with velocity 5.5 km/s to be the initial medium model. Tables 6, 7, and 8 show the solutions with standard errors obtained by the damped least squares method by using Θ defined in (12). As mentioned earlier, the standard errors are based on the conservative overestimate of σ, which is only 5% larger than the correct σ in this case. The epicenters shown in Table 6 are slightly but sometimes significantly shifted to the west from the true location. But the shift is only 0.1 to 0.3 km, which is 1 order of magnitude smaller than the shift in the solution obtained by the use of HYPO71. This slight shift was caused in our case because of a slight overdamping of the slowness perturbation in the peripheral blocks. The residuals unaccounted for by the overdamped medium are forced into the bias in the epicenter location.

The slowness perturbation shown in Tables 7 and 8 obtained by the damped least squares method is much smoother than that obtained by the undamped. Their standard errors range from 1 to 3%. Unlike the undamped solution, the damped one shows smaller values near the periphery than the interior of the area. Except for some peripheral blocks, the result obtained by the damped least squares using the particular choice of weight matrix is quite satisfactory, agreeing well with the true slowness distribution.

The diagonal elements of the resolution

Table 16. Hypocenter (X, Y, Z), Origin Time, and rms Error of the 32 Selected Earthquakes as Located by HYPO71 Using a Regional Model and by HYPO74 Using a Local Model

Event	Number of Stations	Case 1: Regional Model					Case 2: Local Model				
		X	Y	Z	Origin Time	rms Error	X	Y	Z	Origin Time	rms Error
1	35	3.64	39.91	6.59	31.84	0.24	6.46	40.05	5.19	31.57	0.09
2	36	5.92	13.61	8.38	56.63	0.17	10.12	12.78	8.74	56.27	0.04
3	11	6.05	13.94	8.48	11.40	0.16	9.95	12.87	9.20	10.99	0.03
4	17	7.32	34.70	7.31	30.03	0.21	11.20	35.32	6.94	29.68	0.12
5	30	7.73	35.16	6.43	51.09	0.18	10.86	35.15	7.02	50.68	0.09
6	11	6.91	35.03	7.24	30.89	0.22	10.44	35.74	6.36	30.63	0.18
7	14	12.55	4.46	9.51	33.58	0.15	16.43	4.27	6.04	33.25	0.13
8	38	7.71	34.49	6.63	27.22	0.20	11.01	34.94	7.14	26.81	0.09
9	39	6.05	25.46	5.51	26.90	0.23	9.79	25.87	4.63	26.64	0.16
10	46	6.94	7.89	4.55	45.12	0.19	10.62	7.07	2.77	44.84	0.02
11	51	6.87	7.47	5.33	56.12	0.20	10.62	6.67	1.63	55.87	0.03
12	41	7.02	7.82	4.12	20.52	0.20	10.58	6.68	1.77	20.25	0.02
13	17	6.05	21.12	5.84	9.18	0.15	9.57	20.67	7.41	8.77	0.03
14	48	6.90	10.91	5.95	16.95	0.12	10.68	10.37	6.15	16.64	0.03
15	45	8.31	24.95	4.45	45.52	0.20	11.82	25.20	3.80	45.18	0.07
16	52	15.59	10.63	13.14	20.04	0.16	20.16	8.43	8.09	20.03	0.15
17	50	6.05	14.86	5.77	58.91	0.20	10.27	14.67	6.38	58.58	0.03
18	27	6.42	14.46	7.16	49.45	0.17	10.24	14.19	6.54	49.22	0.03
19	8	6.64	8.62	5.00	39.95	0.20	10.20	7.81	1.62	39.73	0.04
20	55	6.63	15.86	5.61	45.49	0.17	10.27	14.74	6.26	45.17	0.03
21	55	6.47	16.15	6.04	45.31	0.19	10.35	15.25	6.32	44.99	0.03
22	54	6.60	16.24	6.61	24.46	0.19	10.27	15.32	6.53	24.15	0.03
23	52	6.47	15.35	5.91	1.73	0.17	10.29	14.49	6.33	1.38	0.03
24	48	6.50	15.34	5.59	53.49	0.17	10.34	14.73	6.46	53.14	0.03
25	38	6.90	15.52	6.17	57.62	0.15	10.32	14.77	5.36	57.36	0.03
26	48	5.94	14.78	7.38	37.21	0.16	10.01	14.02	8.22	36.85	0.03
27	54	6.22	25.22	5.52	3.83	0.20	9.40	25.25	5.21	3.53	0.05
28	51	5.42	31.32	5.00	29.79	0.25	8.55	31.36	1.53	29.58	0.08
29	48	15.50	3.80	11.60	30.50	0.19	19.49	2.11	5.02	30.51	0.14
30	25	15.41	3.53	11.43	12.58	0.18	20.00	3.07	4.38	12.51	0.18
31	37	6.35	13.52	7.77	40.07	0.16	10.20	12.94	6.95	39.78	0.03
32	37	5.97	29.82	5.30	21.30	0.25	8.98	30.23	1.69	21.03	0.06

Here X, Y, and Z are in kilometers, and the origin times and rms errors are in seconds.

matrix corresponding to the above solution are shown in Tables 9, 10, and 11. The resolution is very poor for blocks in the extreme periphery, where the damped least squares solution gave overly damped small values. In general, blocks with the diagonal elements greater than about 0.5 appear to give reasonable results.

We have tried the damped least squares with several different Θ from those given in (12). We found a general rule that if we overdamp a particular parameter having an incorrect initial value, then bias is forced on the solution for other parameters. For example, if we increase the value of θ_i for the slowness perturbation, the correction to the initial homogeneous model is restricted, and the result is a greater westward shift of epicenters from the fault.

The effect of the choice of Θ is thus predictable, but the effect of assumed initial earthquake location is very difficult to assess. Different initial locations lead to different block combinations sampled along a particular ray and then to different basic equations (1). Our data set 3 was particularly vulnerable to a wrong choice of initial earthquake location. We applied the damped least squares method with the same Θ as given in (12) but with the initial earthquake location obtained by the HYPO71 as shown in Table 2. The resultant solutions with standard errors are given in Tables 12, 13, and 14. Although the corrections to source parameters put the epicenters and focal depths closer to the true ones, the slowness perturbation is drastically distorted. The result suggests the importance of iterating the inversion process by using the corrected locations as the new initial locations. As we shall see later, the dependence of the solution on the initial earthquake locations was not so severe in the actual case of the Bear Valley data.

We recognize that small standard errors of slowness perturbation given for interior blocks in Table 13 do not reflect the departure of solutions from the true values. The resolution matrix shows diagonal elements close to unity for these blocks (similar to the ones shown in

Table 17. Diagonal Element of Resolution Matrix R, Correction Δ, and Standard Error ε, for Source Parameters of the 32 Earthquake, Events of Case 1

	X km			Y km			Z km			T se		
Event	R	ΔX	ε	R	ΔY	ε	R	ΔZ	ε	R	ΔT	ε
1	0.98	-3.68	0.91	0.95	-0.11	0.62	0.98	-7.25	1.08	0.13	0.28	0.10
2	1.00	-0.11	0.45	1.00	-0.62	0.17	1.00	-1.53	0.62	0.95	0.23	0.09
3	0.99	0.17	0.68	1.00	-0.73	0.40	0.99	-0.45	1.02	0.85	0.14	0.15
4	0.99	-1.30	0.62	0.97	1.81	0.96	0.98	-1.02	0.79	0.33	-0.05	0.18
5	0.99	-2.72	0.62	0.96	-0.11	0.96	0.99	-2.44	0.68	0.32	0.22	0.18
6	0.99	-1.76	0.68	0.96	2.38	0.85	0.98	-1.64	0.85	0.24	-0.07	0.16
7	0.99	0.45	0.62	0.99	-1.87	0.62	0.98	-0.40	1.08	0.69	-0.07	0.18
8	0.99	-2.15	0.57	0.98	1.64	0.96	0.99	-0.85	0.74	0.55	-0.08	0.20
9	1.00	-0.90	0.40	1.00	1.87	0.34	1.00	-1.36	0.57	0.94	0.01	0.10
10	1.00	0.62	0.28	1.00	-0.51	0.23	1.00	-1.98	0.45	0.98	0.21	0.06
11	1.00	0.45	0.28	1.00	-0.62	0.23	1.00	-3.85	0.40	0.97	0.28	0.06
12	1.00	0.51	0.28	1.00	-0.79	0.17	1.00	-2.21	0.40	0.98	0.22	0.05
13	1.00	0.40	0.51	1.00	0.51	0.28	0.99	-0.51	0.85	0.91	0.24	0.12
14	1.00	0.57	0.23	1.00	-0.11	0.17	1.00	-0.91	0.45	0.97	0.25	0.06
15	1.00	0.23	0.28	1.00	-0.23	0.23	1.00	-2.78	0.45	0.98	0.41	0.06
16	1.00	-1.02	0.28	1.00	-2.38	0.28	0.99	-0.51	0.85	0.86	0.19	0.13
17	1.00	1.25	0.28	1.00	0	0.11	1.00	-1.02	0.45	0.98	0.28	0.06
18	1.00	0.57	0.34	1.00	-0.06	0.17	0.99	-1.70	0.68	0.95	0.30	0.09
19	1.00	0.28	0.62	1.00	-0.79	0.51	0.96	-3.23	1.76	0.82	0.27	0.16
20	1.00	0.28	0.23	1.00	-0.96	0.11	1.00	-0.79	0.40	0.98	0.26	0.05
21	1.00	0.45	0.23	1.00	-0.85	0.11	1.00	-0.90	0.45	0.98	0.23	0.06
22	1.00	0.17	0.23	1.00	-0.79	0.11	1.00	-0.85	0.45	0.98	0.18	0.06
23	1.00	0.68	0.23	1.00	-0.68	0.11	1.00	-0.79	0.45	0.98	0.20	0.06
24	1.00	0.62	0.23	1.00	-0.40	0.11	1.00	-0.62	0.45	0.98	0.23	0.06
25	1.00	0.45	0.28	1.00	-0.62	0.17	1.00	-1.87	0.57	0.97	0.28	0.07
26	1.00	0.28	0.28	1.00	-0.51	0.17	1.00	-0.45	0.51	0.96	0.16	0.08
27	1.00	0.23	0.28	1.00	-0.51	0.28	1.00	-3.62	0.51	0.97	0.47	0.07
28	1.00	0.11	0.40	0.99	-0.85	0.79	0.99	-5.84	0.74	0.77	0.57	0.17
29	1.00	0.62	0.40	0.99	-3.17	0.51	0.98	2.10	0.91	0.75	-0.43	0.16
30	1.00	0.57	0.40	0.99	-1.42	0.62	0.98	-1.08	1.02	0.72	-0.01	0.17
31	1.00	0.62	0.34	1.00	-0.34	0.17	1.00	-2.72	0.62	0.95	0.34	0.09
32	1.00	-0.51	0.45	0.99	-0.40	0.68	0.99	-6.18	0.74	0.84	0.42	0.15

Table 10) and also fails to warn of such a departure. The failure is due to the higher-order terms neglected in the linearization of the basic equation. These nonlinearity effects cannot be measured by the standard error calculated for the effect of random error on the linearized system nor by the resolution matrix, which is essentially a weight function for a linear smoothing.

Application to Bear Valley Data

During the summer of 1974 a detailed monitoring of local earthquakes was carried out in the Bear Valley area of central California by the U. S. Geological Survey under the leadership of J. H. Healy. A multisensor seismic system of 51 elements (nicknamed 'centipede') was deployed [Fischer et al., 1975] together with 14 independently recorded portable instruments. We have selected an area of 24 by 44 km in Bear Valley (see Figure 2) for our applications of the inversion program. The coordinate origin is placed at 36°27.52'N, 121°11.06'W, and sea level, and the Y axis is chosen parallel to the general direction of the San Andreas fault and strike (N43°W) in this area. A generalized geologic map of the study area is shown in Figure 3, which was greatly simplified from detailed mapping by Dibblee [1973, 1975] and Dibblee and Rogers [1975]. The fault zone is about 3 to 7 km wide, bounded by the San Andreas and Calaveras faults.

Within this study area there were 43 'centipede' stations, 9 portable stations, and 8 permanent stations, for a total of 60 stations as listed in Table 15 and shown in Figures 4 and 5. Thirty-two local earthquakes with magnitude greater than 2 were selected among the several hundreds (magnitude ranges from 1 to 3) that were recorded. Selections were made to maximize the number of blocks penetrated by ray paths connecting the hypocenter and station. A total of 1218 first P arrival times were available for inversion.

The crustal model that we used in the inversion for the Bear Valley study area consisted of rectangular blocks. The side lengths of blocks in the X, Y, and Z directions were 3, 4, and 5 km, respectively. Blocks of 8 x 11 x 3 covered the whole volume of the earth under consideration.

Table 18. Diagonal Element of Resolution Matrix R, Correction Δ, and Standard ε, for Source Parameters of the 32 Earthquake, Events of Case 2

	X km			Y km			Z km			T s		
Event	R	ΔX	ε	R	ΔY	ε	R	ΔZ	ε	R	ΔT	ε
1	0.99	-7.82	0.91	0.95	1.98	0.68	0.98	-4.59	1.25	0.13	0.19	0.11
2	1.00	-4.93	0.40	1.00	0.17	0.23	1.00	0.57	0.68	0.95	0.43	0.10
3	1.00	-4.19	0.62	1.00	0.57	0.45	0.99	1.25	1.13	0.87	0.37	0.16
4	1.00	-6.07	0.68	0.97	2.78	1.08	0.98	3.34	1.02	0.34	-0.13	0.20
5	1.00	-7.20	0.68	0.97	0.85	1.13	0.98	2.21	0.91	0.36	0.22	0.21
6	0.99	-6.12	0.68	0.96	2.89	1.02	0.98	3.06	1.02	0.24	-0.20	0.18
7	1.00	-2.27	0.51	1.00	-1.30	0.68	0.99	3.63	1.08	0.85	0.29	0.17
8	1.00	-6.35	0.51	0.98	3.57	1.13	0.98	3.46	0.96	0.52	-0.30	0.23
9	1.00	-4.36	0.34	1.00	0.91	0.34	1.00	0.39	0.68	0.96	0.33	0.09
10	1.00	-3.00	0.23	1.00	0.17	0.23	1.00	1.30	0.51	0.99	0.45	0.05
11	1.00	-3.12	0.23	1.00	0.40	0.17	1.00	1.81	0.57	0.99	0.51	0.05
12	1.00	-3.06	0.23	1.00	0.40	0.17	1.00	1.59	0.57	0.99	0.50	0.05
13	1.00	-3.70	0.40	1.00	1.02	0.34	0.99	-0.74	0.96	0.92	0.54	0.12
14	1.00	-3.46	0.23	1.00	0.34	0.23	1.00	0.91	0.51	0.98	0.43	0.07
15	1.00	-3.86	0.28	1.00	-0.34	0.28	1.00	-0.51	0.74	0.98	0.64	0.07
16	1.00	-3.57	0.40	1.00	0.06	0.28	0.99	5.50	0.85	0.90	0.21	0.13
17	1.00	-3.29	0.23	1.00	0.40	0.17	1.00	-0.06	0.51	0.98	0.51	0.06
18	1.00	-3.29	0.28	1.00	0.34	0.17	1.00	0.27	0.73	0.96	0.47	0.09
19	1.00	-4.31	0.62	1.00	-0.74	0.57	0.84	5.22	3.68	0.85	0.26	0.16
20	1.00	-3.57	0.23	1.00	0.34	0.17	1.00	0.17	0.45	0.98	0.49	0.06
21	1.00	-3.46	0.23	1.00	0.34	0.11	1.00	0	0.45	0.98	0.51	0.06
22	1.00	-3.46	0.23	1.00	0.34	0.17	1.00	-0.06	0.51	0.98	0.51	0.06
23	1.00	-3.34	0.23	1.00	0.34	0.17	1.00	0.17	0.51	0.98	0.49	0.06
24	1.00	-3.40	0.23	1.00	0.40	0.17	1.00	0.11	0.51	0.98	0.49	0.06
25	1.00	-3.29	0.23	1.00	0.40	0.17	1.00	0.34	0.57	0.98	0.46	0.07
26	1.00	-4.20	0.28	1.00	0.40	0.17	1.00	0.45	0.62	0.97	0.44	0.08
27	1.00	-3.34	0.28	1.00	-0.45	0.28	1.00	-2.10	0.57	0.97	0.69	0.08
28	1.00	-3.80	0.34	0.99	-2.44	0.85	0.99	-2.61	0.91	0.87	0.99	0.16
29	1.00	+1.10	0.51	0.99	-4.03	0.74	0.98	14.57	1.25	0.77	-1.22	0.20
30	1.00	-2.15	0.57	1.00	-1.13	0.62	0.99	7.65	1.19	0.85	0.03	0.17
31	1.00	-3.52	0.28	1.00	0.40	0.17	1.00	0	0.62	0.97	-0.51	0.08
32	1.00	-3.91	0.45	0.99	-0.40	0.85	0.99	-1.34	1.02	0.87	0.63	0.16

We also assumed a constant P velocity of 5.67 km/s for all the blocks initially.

Initial source parameters were obtained by locating the selected earthquakes by using the HYPO71 computer program [Lee and Lahr, 1975] and its modified version HYPO74. Two crustal models were used: case 1, the regional model (consisting of three layers over a half space with the thickness of the first layer being a variable under each station) as used for the standard analysis of the U. S. Geological Survey Central California Microearthquake Network [Lee et al., 1972], and case 2, the local model as derived by W. L. Ellsworth for the Bear Valley area.

Since the location programs can only compute travel time and derivatives for flat layer models, they are not applicable to the region where large lateral variations exist. In the regional model we attempted to relax this restriction by assuming different thickness of the first layer for each station. The crustal thickness in the local model is 25 km, the mantle velocity being 8.05 km/s. The velocity in the crust is assumed to be 5.67 km/s in the east side of the fault, while in the west side of the fault, 5.94 km/s is adopted for epicentral distances less than about 35 km, and 6.3 km/s is adopted for greater distances. Station corrections for the local model are determined from the time residuals for sample earthquakes in the Bear Valley area on the assumption that the epicenters lie on the fault. The corrected residuals are all delays relative to the above crustal models and range from 0 to as much as 1.6 s. The initial source parameters obtained in these two cases are listed in Table 16, and epicenters are plotted in Figure 4 for the regional model and in Figure 5 for the local model. The local model gave better hypocenter locations than the regional model in the sense that the rms residual was 0.07 s for the local model versus 0.19 s for the regional model. Since the station corrections in the local model were designed to put epicenters on the San Andreas fault, the epicenters were placed near the fault by using the local model. On the other hand, they were placed about 3 km west of the fault by using the regional model.

The damped least squares method was used for the inversion. The weight matrix Θ was deter-

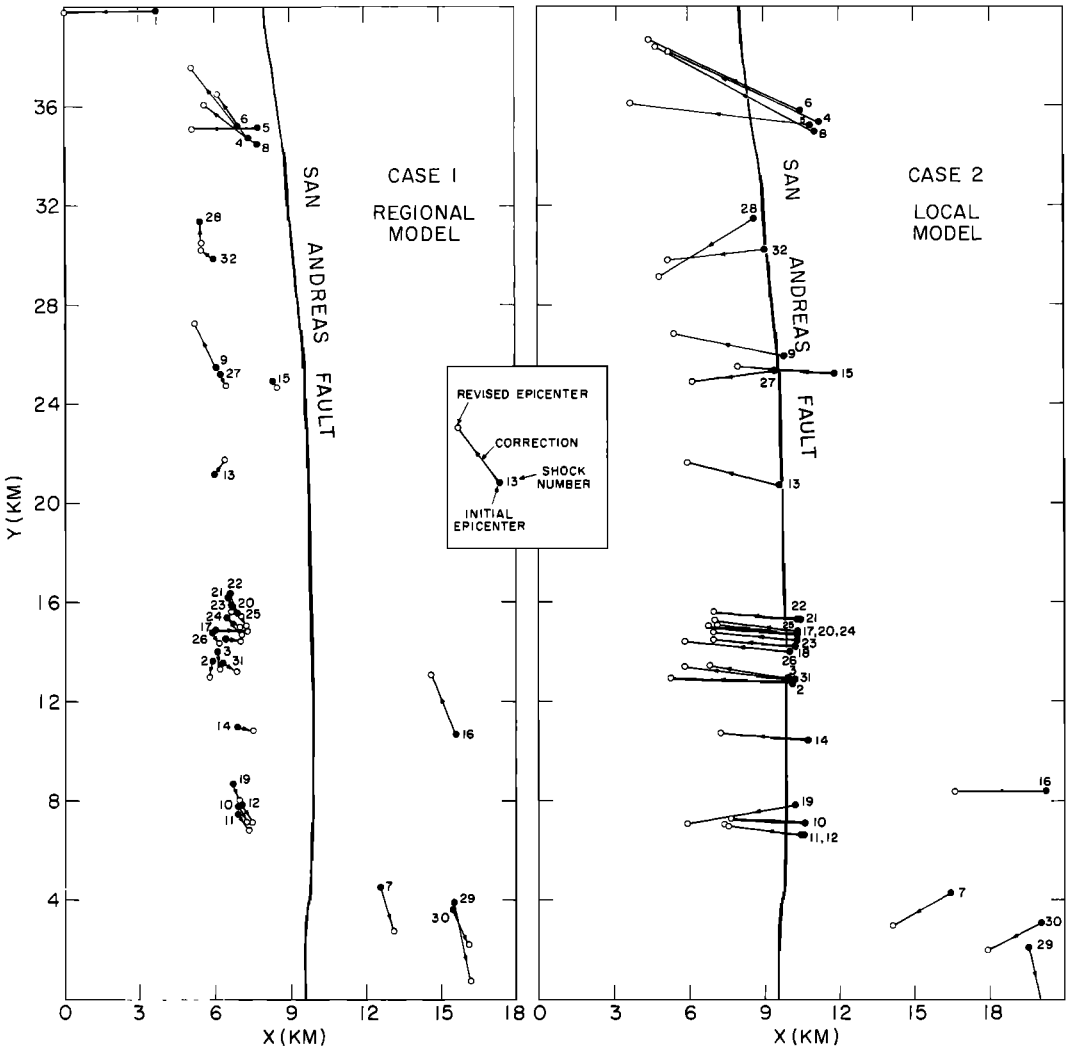

Fig. 6. Comparison of initial epicenters and revised epicenters between cases 1 and 2. Most of the revised epicenters agree within 1 km. The shock numbers correspond to those given in Table 16.

mined by (7) assuming that $\sigma = 0.1$ s, $\sigma_i = 0.05$, $\sigma_x, = \sigma_y = \sigma_z = 10$ km, and $\sigma_T - 0.5$ s. By this choice of Θ the constraint on the source parameters is very weak, so that the bias effect due to constraint on the parameters with incorrect initial values discussed earlier may be minimized. The choice of σ_i 4 times larger than the adopted value (0.05) resulted in unacceptable standard errors. Small values of σ_x, σ_y, σ_z, say, less than 1 km, on the other hand, caused poor resolution for source parameters.

The results of the inversion for source parameters are shown in Tables 17 and 18 and in Figure 6. Table 17 lists the corrections to the initial source parameters for case 1 (regional model). It also gives the diagonal element of resolution matrix and the standard error for each source parameter. Table 18 lists the results for case 2 (local model).

In both cases the resolution for epicenter and focal depth is excellent for all events. The resolution for origin time, however, becomes very poor for events located in the peripheral region, because of the compensation between the origin time and the slowness perturbation of the block containing the hypocenter. The standard errors of focal depth corrections are around 0.5 to 1 km, which is roughly twice as large as those of epicenter coordinates. The standard error of the origin time is about 0.1 s.

The corrections to epicenter locations are compared between case 1 and 2 in Figure 6. The closed circles, arrows, and open circles indicate the initial epicenter, correction, and revised epicenter, respectively. Most of the initial epicenters for case 1 are located about 3 km west of the San Andreas fault, while those for case 2 are located close to the fault. In spite of the difference in the initial locations the revised epicenters for case 1 and 2 are very close to each other, less than 1 km apart for most events. It shows that at least for epicenter locations the solution does not depend on the initial model. We can definitely conclude that the earth's structure in the Bear Valley area is quite different from the simple velocity contrast model (6.0 km/s in the west side and 5.0 km/s in the east side of the San

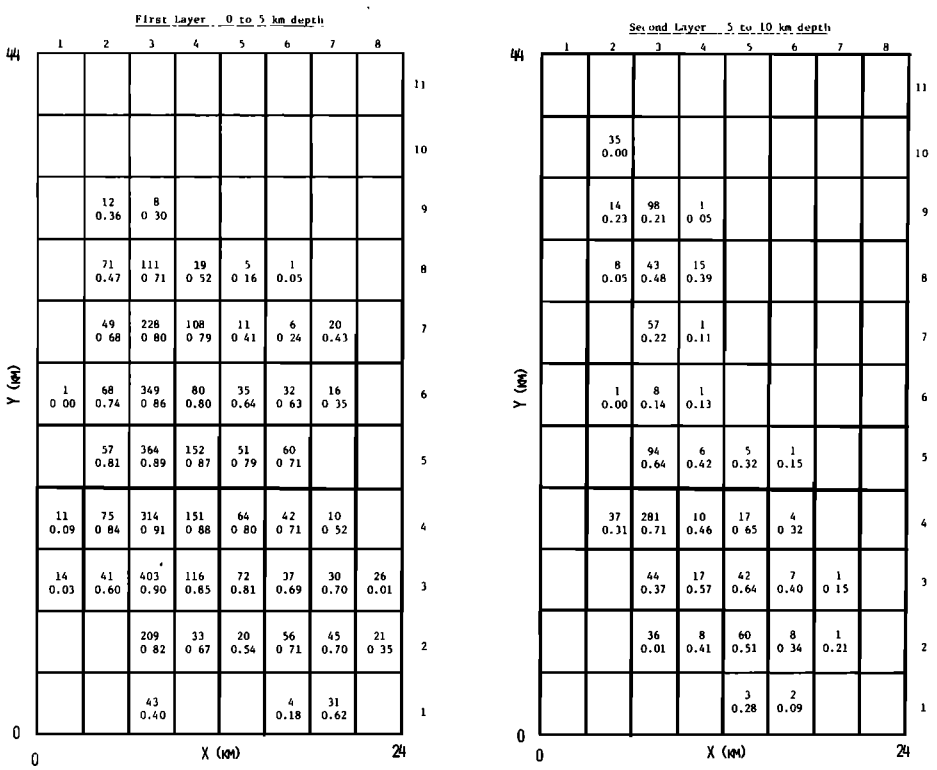

Fig. 7. Number of penetrating seismic rays (upper number) and the diagonal element of resolution matrix (lower number) for case 1.

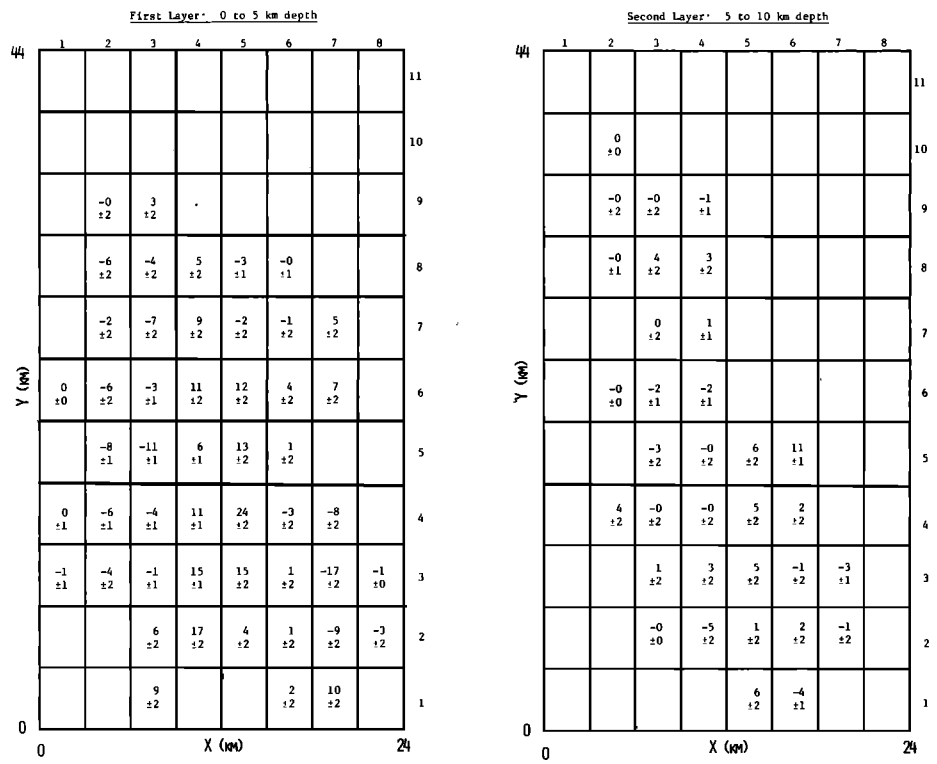

Fig. 8. Perturbation of slowness in percent (upper number) and its standard error (lower number) for case 1.

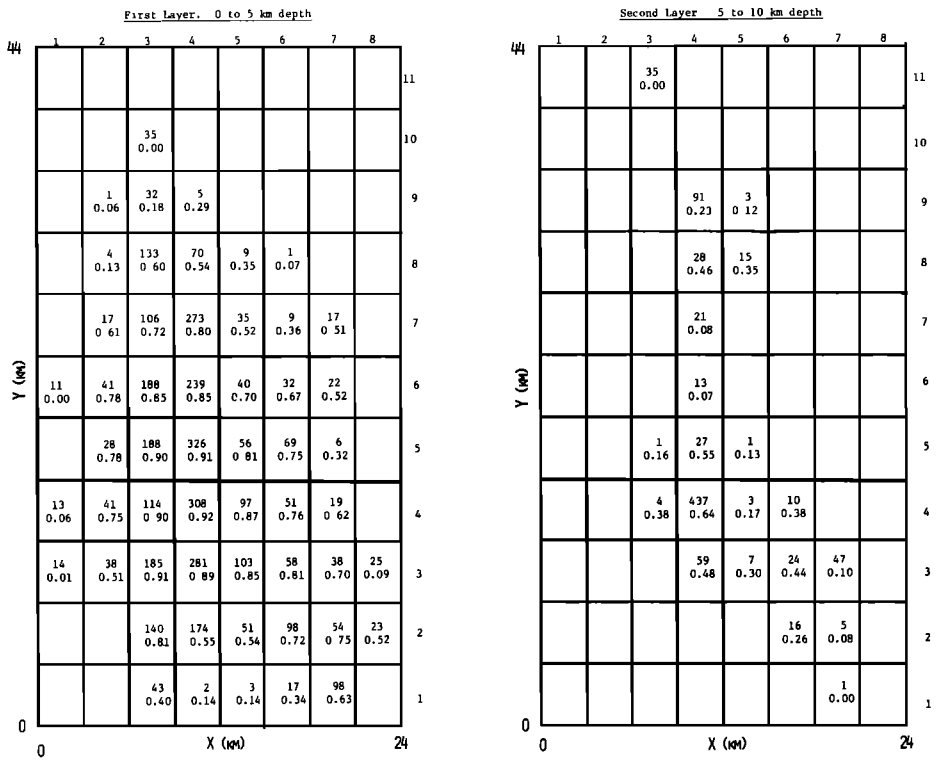

Fig. 9. Number of penetrating seismic rays (upper number) and the diagonal element of resolution matrix (lower number) for case 2.

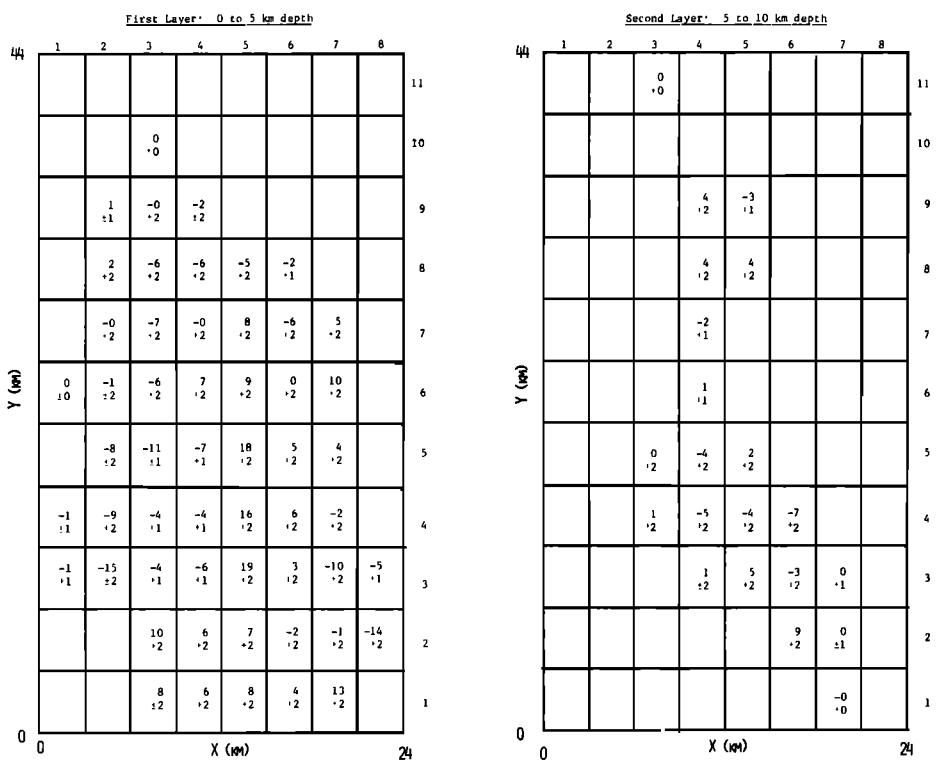

Fig. 10. Perturbation of slowness in percent (upper number) and its standard error (lower number) for case 2.

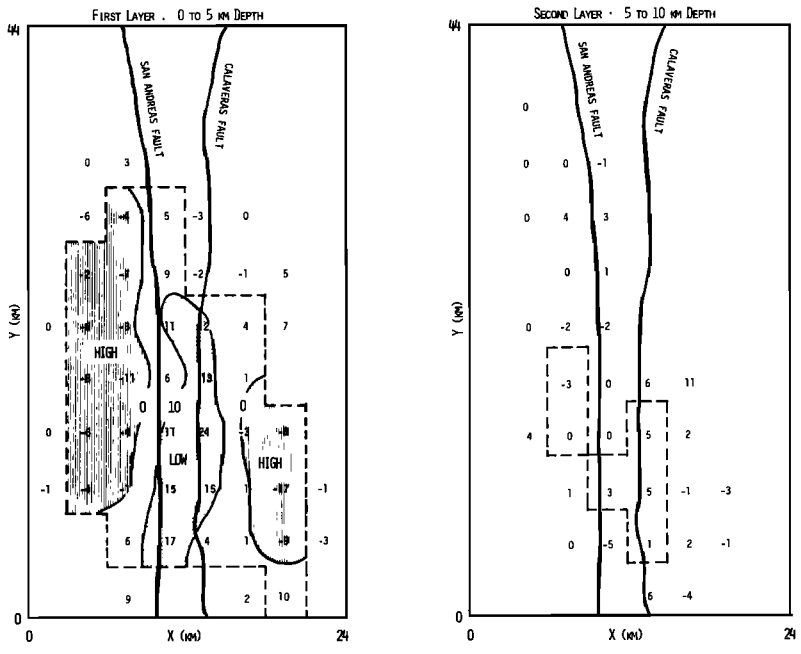

Fig. 11. Map showing contours of slowness in percent (upper number) and its standard error (lower number) for case 2.

Andreas fault) of artificial data set discussed earlier, because in the case of artificial data set 3, no epicenter correction was required when the initial location was on the fault, and a considerable eastward correction was required when the initial location was about 2.5 km west of the fault.

The resultant revised epicenter locations are, however, very disturbing. They do not line up with the fault but are placed about 3 km west of the fault. In other words, the correction to the initial epicenters for case 1 was insignificant, and the correction for case 2 approximately reproduced the initial epicenters for case 1. Thus the residuals absorbed in the station correction in case 2 (restricting epicenter on the fault) cannot be explained by a physical model of three-dimensional velocity variation without the westward shift of the epicenter. Thus we reach an inevitable conclusion that the epicenters are located about 3 km west of the San Andreas fault. This conclusion is, however, conditional because of our homogeneous initial model. Strong refractions introduced by lateral velocity change may produce a systematic bias in our solution. For a definitive conclusion we must obtain the solution iteratively by using ray tracing in a heterogeneous medium. Since we do not yet have an effective ray tracing program, no iteration was made. However, progress has been made on relocating local eqarthquakes by using seismic ray tracing [Engdahl and Lee, 1976]. It is possible to iterate the inversion by using the revised source parameters and the same homogeneous initial model. But such an iteration for case 1 would produce the same result as the first inversion because the correction to source parameters was insignificant. The iteration for case 2 will generate the result similar to that of case 1, because the revised source parameters for case 2 are similar to the initial source parameters for case 1.

Another possible cause of the bias is overly heavy damping of slowness fluctuations as demonstrated earlier by using an artificial data set. If the westward shift of the epicenter from the fault is due to the heavy damping, the actual velocity distribution must be much more strongly variable than our solutions shown below. In that case, we need a denser station network to make the block size smaller so that stronger heterogeneity can be properly treated.

Now, let us show the results of the inversion for medium parameters in Figures 7-12. For each block penetrated by at least one ray path we shall give the slowness perturbation (the parameter F_k of (1), its standard error, the diagonal element of the resolution matrix, and the number of ray paths penetrating the block.

Figure 7 shows the number of ray paths through each block (upper number) and the diagonal element of resolution matrix for case 1 (lower number). Resolution for slowness perturbation is good for blocks of the first layer except for the peripheral region. Resolution for the second layer is poor except for the central area. We neglected the third layer because only a few blocks are sampled there. Figure 8 shows the slowness perturbation in percent (upper number) and its standard error (lower number) for case 1. Values of slowness perturbation are in the range of -7 to +24%, whereas the standard errors are typically 2 %. Therefore most slowness perturbations are statistically significant unless they suffer from the nonlinearity effect discussed earlier. Results for case 2 are similar to those for case 1 as shown in Figures 9 and 10.

Contour maps of slowness perturbations are

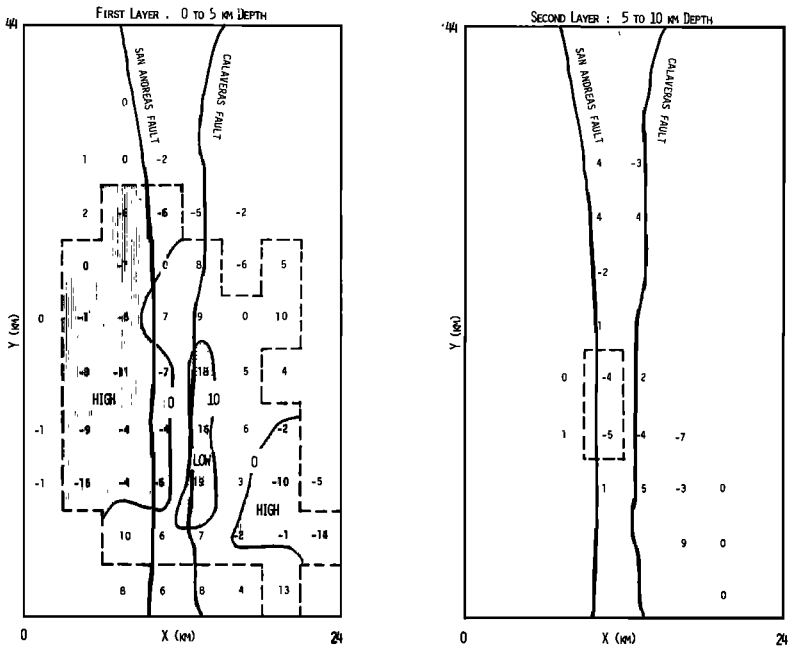

Fig. 12. Map showing contours of slowness perturbation in percent for case 2. Blocks enclosed by the dashed lines have the diagonal element of resolution matrix greater than or equal to 0.5.

shown in Figure 11 for case 1 and in Figure 12 for case 2. In drawing the contours we considered only those blocks enclosed by dashed lines, for which the diagonal element of resolution matrix exceeds 0.5. Areas with negative slowness perturbation are marked 'high' velocity, and areas with positive slowness are marked 'low.' Since the average velocity is assumed as 5.67 km/s (slowness 0.716 s/km), 6% 'high' corresponds to 6.06 km/s (slowness 0.165) and 15% 'low' corresponds to 4.95 km/s (slowness 0.202). The general pattern of velocity perturbations in the first layer is common to both cases 1 and 2: a low-velocity zone of about 5 km/s in the San Andreas fault zone, sandwiched between high-velocity areas of about 6 km/s.

The details of the contour map, however, differ between the two cases, although the differences are not as pronounced as those in artificial data set 3 discussed earlier. The low-velocity zone is wider for case 1 than for case 2, although in both cases the peak occurs along the part of the Calaveras fault where serpentine is exposed. Geologically, the result for case 1 is preferred to that for case 2, because in the latter the high-velocity area appears to invade the fault zone filled with Quaternary sediments.

We also consider the result for case 1 more satisfactory than that for case 2 for the following two reasons. First, the fit to observed residuals for case 1 was better than that for case 2. The rms residual was 0.086 s for case 1 and 0.098 s for case 2. Second, since the revised epicenters of case 2 were close to the initial epicenters of case 1, further iteration of inversion with the revised epicenters of case 2 would have generated a result similar to that of case 1. The importance of such an iteration was emphasized earlier in the case of artificial data set 3.

Our result shows some discrepancy with the velocity distribution across the Bear Valley area obtained by Wesson [1971]. Wesson applied an iterative linear inversion method including ray tracing in a heterogeneous medium to travel time data obtained at a temporary seismometer array from a single explosion located in Bickmore Canyon. The discrepancy is that the main feature of Wesson's velocity anomaly is a smooth transition from the high velocity on the west to the low velocity on the east, rather than a narrow low-velocity zone as obtained in our result. This discrepancy may be due to the artifact of smooth functions used to model the velocity distribution by Wesson, but we cannot deny the possibility that the discrepancy may be due to the oversimplified initial medium model used in our inversion method. The discrepancy also may be due to the difference in the amount of data; Wesson used 13 readings from a single shot, whereas we used 1218 readings from 32 shocks.

Healy and Peake [1975] recently published a paper summarizing the data from four earthquakes in the Bear Valley area acquired by the 24 permanent stations distributed in the area within about 50 km of the Bear Valley supplemented by 27 portable stations and 30 array stations operated during March 1972. The isochron maps of first arrivals at these stations demonstrate the strong lateral inhomogeneity in the area. The apparent center of the smallest isochron is located about 3-4 km off to the west of the fault. By using only data obtained from the stations on the granite of the Gabilan range the epicenter was brought closer to the fault but was still off to the west of the fault by 1-2 km. Their proposed

tentative crustal model shows a low-velocity fault zone sandwiched by high-velocity regions, roughly similar to our result.

Coming back to our results shown in Figures 11 and 12, although we do not have sufficient data to contour the second layer (depths of 5 to 10 km), both solutions suggest that the velocity anomalies are much smaller than those in the first layer and the low-velocity zone found in the top layer does not extend to the second layer.

Discussion

Under the restriction of a homogeneous initial earth model we found that epicenters in the Bear Valley area are located about 3 km west of the San Andreas fault (Figure 6) and that a low-velocity zone (about 5 km/s) exists at depths of 0 to 5 km, roughly coinciding with the zone between the San Andreas and Calaveras faults (Figure 11).

These conclusions are not definitive because our simplified initial earth model may introduce bias in the solution. This restriction cannot be removed without incorporating ray tracing through a heterogeneous medium into an iterative inversion process.

Another limitation is the availability of high-quality P arrival data for local earthquakes from a dense seismic array. The block size of our Bear Valley model was determined by the station spacing of the seismic array. To resolve complex geology near the fault zone, one would need station spacing of probably less than 1 km, so that hundreds of stations are required even for a small segment of the San Andreas fault such as the Bear Valley area.

Despite the above limitations, we are encouraged by our preliminary results, because they give us remarkably good precision and spatial resolution with which we can determine the seismic velocity anomalies from the currently available data set of local earthquakes. A systematic approach toward earthquake prediction by using local earthquake data may be possible by designing seismic experiments for given conditions on the frequency and magnitude of target earthquake, frequency and spatial distribution of microearthquakes usable as data for inversion, and expected magnitude and spatial extent of precursory velocity change.

Acknowledgments Discussions with Bill Ellsworth at the inception of the present work helped us to recognize the importance of simultaneous determination of source and medium parameters for local earthquakes. We thank Dave Hill for pointing out an error in a formula in an early draft of the paper. Jack Evernden, Dave Hill, Sam Stuart, and George Zandt read the draft and suggested improvements. The paper was extensively revised to respond to the constructive criticism of R. S. Crosson, who reviewed the paper. This work was supported partially by the U. S. Geological Survy under contract 14-18-0001-14889; publication was authorized by the director of the U. S. Geological Survey.

References

Aki, K., A. Christoffersson, and E. Husebye, Determination of the three-dimensional seismic structure of the lithosphere, submitted to J. Geophys. Res., 81, in press, 1976.

Backus, G. E., and J. F. Gilbert, The resolving power of gross earth data, Geophys. J. Roy. Astron, Soc., 16, 169-205, 1968.

Crosson, R. S., Non-linear least squares crustal structure estimation from earthquake data (abstract), Eos Trans. AGU, 56, 1145, 1974.

Dibblee, T. W., and T. H. Rogers, Geologic map of the Hollister Quadrangle, California, open-file map, U. S. Geol. Surv., 1975.

Dibblee, T. W., Geologic map of the Gonzales quadrangle, California, open-file map, U. S. Geol. Surv., Reston, Va., 1973.

Dibblee, T. W., Geologic map of the San Benito Quadrangle, California, open-file map, U. S. Geol. Surv., Reston, Va., 1975.

Engdahl, E. R., and W. H. K. Lee, Relocation of local earthquakes by seismic ray tracing, J. Geophys. Res., 81, in press, 1976.

Fischer, F. G., S. W. Stewart, and J. H. Healy, Short term multi-sensor seismic system (abstract), Geol. Soc. Amer. Abstr. Programs, 7 (3), 405-406, 1975.

Franklin, J. N., Well-posed stochastic extensions of ill-posed linear prblems, J. Math Anal. Appl., 31, 682-716, 1970.

Healy, J. H., and L. G. Peake, Seismic velocity structure along a section of the San Andreas fault near Bear Valley, California, Bull. Seismol. Soc. Amer., 65, 1177-1198, 1975.

Lee, W. H. K., J. C. Roller, P. G. Bauer, and J. D. Johnson, Catalog of earthquakes along the San Andreas fault system in central California for the year 1969, Open file report, U. S. Geol. Surv., Reston, Va., 1972.

Lee, W. H. K., and J. C. Lahr, HYPO71 (Revised): A computer program for determining hypocenter, magnitude, and first motion pattern of local earthquakes, Open-file report, 75-311, 113 pp., U. S. Geol. Surv., Reston, Va., 1975.

Levenberg, K., A Method for the solution of certain non-linear problems in least squares, Quart. Appl. Math., 2, 164-168, 1944.

Wesson, R. L., Travel-time inversion for laterally inhomogeneous crustal velocity models, Bull. Seismol. Soc. Amer., 61, 729-746, 1971.

Wiggins, R. A., The general linear inverse problem: Implication of surface waves and free oscillations for earth structure, Rev. Geophys. Space Phys., 10, 251-285, 1972.

Zandt, G., Personal communication, 1975.

(Received September 23, 1975;
Accepted March 29, 1976.)